Title	Rotational and vibrational state distribution of H_2 activated on a heated tungsten filament
Author(s)	Umemoto, Hironobu; Ansari, S. G.; Matsumura, Hideki
Citation	Journal of Applied Physics, 99(4): 043510-1-043510-6
Issue Date	2006-02-22
Type	Journal Article
Text version	publisher
URL	http://hdl.handle.net/10119/4523
Rights	Copyright 2006 American Institute of Physics. This article may be downloaded for personal use only. Any other use requires prior permission of the author and the American Institute of Physics. The following article appeared in Hironobu Umemoto, S.G. Ansari, and Hideki Matsumura, Journal of Applied Physics, 99(4), 043510 (2006) and may be found at http://link.aip.org/link/?JAPIAU/99/043510/1
Description	

Rotational and vibrational state distributions of H$_2$ activated on a heated tungsten filament

Hironobu Umemoto,[a)] S. G. Ansari, and Hideki Matsumura

School of Materials Science, Japan Advanced Institute of Science and Technology, Asahidai, Nomi, Ishikawa 923-1292, Japan

The rotational and vibrational state distributions of H$_2$ activated on a heated tungsten filament were determined by employing a coherent anti-Stokes Raman scattering technique to examine the contribution to the catalytic chemical vapor deposition process. The rotational excitation could be confirmed and the distribution was Boltzmann-like. When the filament temperature was 2700 K and the H$_2$ pressure was over 1.3 kPa, the rotational temperature monitored 5 cm under the filament was around 1200 K; it showed a sharp decrease below 670 Pa and it was 700 K at 67 Pa. This decrease in the rotational temperature suggests the importance of relaxation processes on the chamber walls. The first vibrationally excited H$_2$ molecules could also be identified at pressures over 670 Pa and the vibrational temperature was not much different from the rotational one. This vibrational temperature is much lower than those in typical H$_2$ plasma, showing that the direct vibrational excitation of H$_2$ on hot filaments is inefficient compared to its dissociation to two H atoms. © *2006 American Institute of Physics.* [DOI: 10.1063/1.2173044]

I. INTRODUCTION

One of the merits of catalytic chemical vapor deposition (Cat-CVD, often called hot-wire CVD or hot filament CVD), compared with conventional plasma-enhanced CVD (PECVD), is the absence of charged species, such as ions and electrons, in the gas phase. With Cat-CVD, it is possible to prepare thin films without plasma damage.[1–3] Plasma damage can also be avoided in remote PECVD, in which the discharge and the deposition areas are separated.[4,5] One of the possible differences between remote PECVD and Cat-CVD is the contribution of metastable excited species. For example, metastable N($2\,^2D_J$) and N$_2$($A\,^3\Sigma_u^+$), and possibly N$_2$($a'\,^1\Sigma_u^-$), can initiate reactive processes in nitrogen after glow.[6–8] However, none of the excited states of H or H$_2$ are metastable, except for H($2\,^2S_{1/2}$) and H$_2$($c\,^3\Pi_u, \nu=0$).[9] Since the electronic energies of H($2\,^2S_{1/2}$) and H$_2$($c\,^3\Pi_u, \nu=0$) are much higher than the dissociation energy of the H–H bonds, it may react with H$_2$ molecules to rapidly produce two H atoms in the presence of H$_2$. H($2\,^2S_{1/2}$) may also be collisionally relaxed to short-lived $2\,^2P_J$ resonance states easily. Then, the active species in remote plasma processes of H$_2$ and those in catalytic activation may be similar; H($1\,^2S_{1/2}$) and vibrationally excited H$_2$($X\,^1\Sigma_g^+$) should be the only active species in these systems. One of the differences is in the H-atom population. In general, the population of H atoms in catalytic decomposition is higher than in plasma decomposition,[10–12] although high-density H atoms can also be obtained by plasma under some conditions.[4,13–16] In addition, there may also be a difference in the vibrational state distributions of H$_2$. Vibrationally excited H$_2$ may be another key species in discussing the difference between PECVD, both remote and conventional, and Cat-CVD. In general, the reaction rate constant increases with vibrational excitation.

Especially, the vibrational quantum of H$_2$ is large and the effect is large. For example, the vibrational excitation of H$_2$ increases the rate constants for O($2\,^3P_J$)+H$_2$ and OH($X\,^2\Pi_J$)+H$_2$ by more than two orders of magnitude.[17,18]

The rotational and vibrational state distributions of H$_2$ after plasma excitation have been extensively characterized.[19–26] The vibrational temperatures are, in general, more than 2000 K and the distribution is non-Boltzmann for highly excited levels. The rotational distributions are not necessarily Boltzmann-like either but are generally cooler than the vibrational ones. The excitation of H$_2$ on heated filaments, on the other hand, has been studied less extensively,[12,27–29] and few studies have reported on vibrational excitation. Hall and co-workers have shown that highly vibrationally excited H$_2$ molecules are produced in hot filament excitation.[27,29] They monitored H$^-$ ions formed by the dissociative attachment of electrons to H$_2$ molecules. This technique is sensitive for detecting highly vibrationally excited H$_2$ but is less sensitive for vibrational ground-state and first-excited-state H$_2$.

In the present study, the rotational and vibrational state distributions of H$_2$ were examined after excitation on heated tungsten filaments. Since the most populated excited state must be the lowest one, H$_2$($\nu=1$), a coherent anti-Stokes Raman scattering (CARS) technique was employed to determine the populations of the $\nu=0$ and $\nu=1$ levels, where ν is the vibrational quantum number. Other techniques, such as laser-induced fluorescence (LIF) and resonant-enhanced multiphoton ionization (REMPI), are sensitive to detect highly vibrationally excited H$_2$ but are hard to apply to $\nu=0$ and $\nu=1$ levels. Recently, we have reported that vibrationally excited CN radicals, CN($\nu=1$), can be identified in the catalytic decomposition of HCN.[30] The vibrational temperature was 1900 K when the filament temperature was 2300 K. If this is the case, the vibrational population ratio

---

a)Electronic mail: umemoto@jaist.ac.jp

99, 043510-1

$[H_2(\nu=1)]/[H_2(\nu=0)]$ should be 0.04, which is comparable to that observed in typical plasma processes. Although no vibrationally excited states have been observed for SiH and NH in the decomposition of SiH_4 and NH_3, respectively, these species may not be the nascent products on the catalyzer surfaces.[31,32]

II. EXPERIMENT

A conventional CARS technique was employed to determine the rotational and vibrational state distributions of H_2.[33,34] The vacuum and laser systems were similar to those described elsewhere.[10,30–32,35,36] A resistively heated tungsten wire (Nilaco 99.95%, 0.5 mm in diameter, and 170 cm in length) was used to activate flowing molecular hydrogen in a vacuum chamber with a 45 cm internal diameter that was evacuated with a turbomolecular pump through a butterfly valve. The distance between the filament and the showerhead was 19 cm while that from the chamber bottom was 12 cm. The shortest distance between the filament and the chamber sidewalls was 10 cm. The flow rate of H_2 was fixed at 100 SCCM (standard cubic centimeter per minute) (1 SCCM $=6.9\times10^{-7}$ mol s^{-1}) while the pressure was changed between 27 Pa and 2.7 kPa by adjusting the butterfly valve. In CARS measurements, the second harmonic of a Q-switched neodymium-doped yttrium aluminum garnet (Nd:YAG) laser (Spectra Physics PRO-190-10) at 532 nm was split into two parts. One part was used to pump a dye laser (Lumonics HD-500) whose output around 684 nm was used as the tunable Stokes beam ω_S. The Stokes pulse energy was 6 mJ. The remaining part, 10 mJ/pulse, was used directly as the pump beam ω_P. CARS spectra were recorded by monitoring the intensity of the anti-Stokes signal beam $\omega_{AS}=2\omega_P-\omega_S$ around 435 nm. The pump and the Stokes beams were combined, made collinear at a beam combiner (dichroic mirror), and focused into the chamber using a 400 mm focal length achromatic lens. The pump beam was optically delayed for proper temporal overlap with the dye laser beam. The anti-Stokes signal was separated from the pump and the Stokes beams with a Pellin-Broca prism and was detected with a photomultiplier tube (Hamamatsu Photonics R212UH) through two glass filters (Toshiba V-42 and C-40C) and a monochromator (JASCO CT25C). The slits of the monochromator were widely opened to ensure the wavelength independence of the detection sensitivity. This was checked by monitoring the nonresonant CARS signals in air. Neutral density filters were used when necessary. The photomultiplier signal was amplified and processed with a boxcar averager-gated integrator system (Stanford Research Systems SR240/SR250/SR280) and was transferred to a computer (IBM PC300PL). The wave number of the dye laser output was checked with a wave meter (Burleigh VA-5500). The typical filament temperature was 2700 K, while the distance between the filament and the detection zone was 5 cm. H_2 (Takachiho 99.999 95%) was used from a cylinder without further purification.
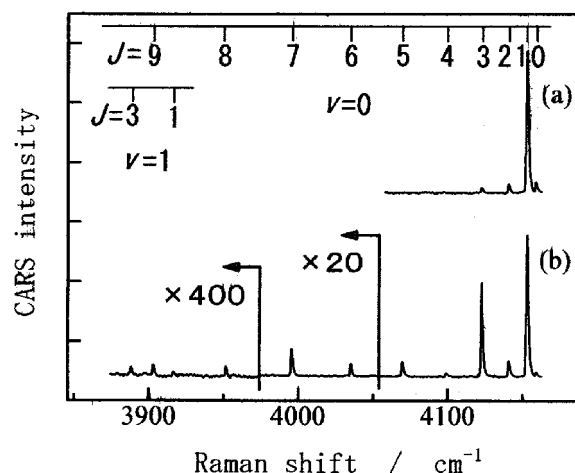

FIG. 1. Q-branch CARS spectra of H_2. (a) H_2 pressure of 1.3 kPa without heating the filament; (b) H_2 pressure of 2.7 kPa with heating the filament up to 2700 K. The distance between the filament and the detection zone was 5 cm. The wavelength dependence of the Stokes laser intensity has been corrected.

III. RESULTS

Figure 1 shows typical CARS spectra when the filament was heated and unheated. When the filament was heated up to 2700 K, rotational levels up to $J=9$ could be observed for the vibrational ground state, where J is the rotational quantum number. Vibrationally excited hydrogen, $H_2(\nu=1)$, could also be identified for $J=1$ and $J=3$, although the signal intensities were three orders of magnitude weaker than those for $H_2(\nu=0)$. Figure 2 illustrates the H_2 pressure dependence of the square root of the CARS signal intensity, showing the absence of signal saturation. Figure 3 shows the Boltzmann plots of the rotational distributions of $H_2(\nu=0)$ obtained under three conditions. In this figure, the logarithm of the square root of the Raman signal intensity divided by the rotational degeneracy, $2J+1$, nuclear spin degeneracy, 1 or 3, and the J dependent part of the third-order nonlinear susceptibility, $6+J(J+1)/(2J-1)(2J+3)$,[28] is plotted against the rotational energy. The three plots in Fig. 3 are all linear, suggesting that the rotational distributions are Boltzmann-like.
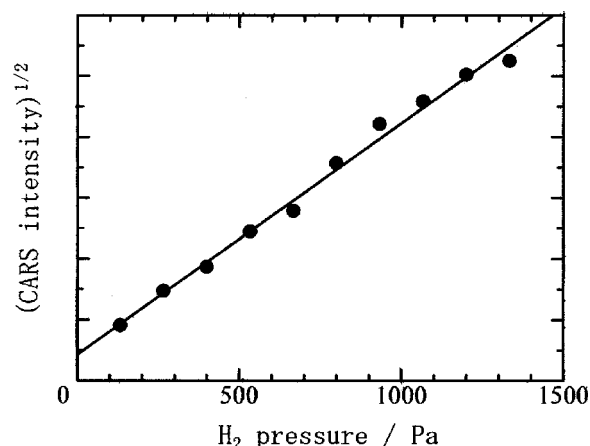

FIG. 2. Square root of the CARS signal intensity of $H_2(\nu=0,J=3)$ as a function of H_2 pressure. The filament temperature was 2300 K. The intercept corresponds to the off-resonant CARS signal caused by air.
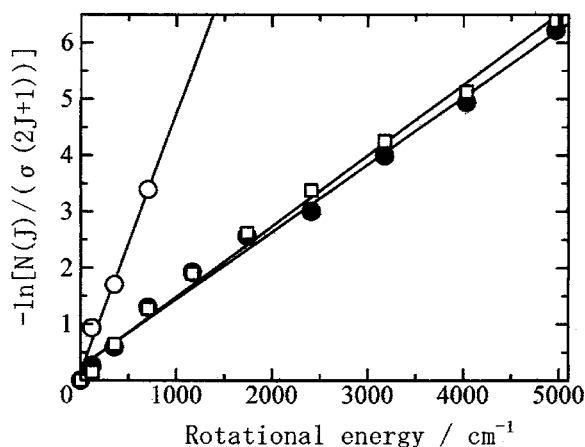
FIG. 3. Rotational Boltzmann plots of $H_2(\nu=0)$. The H_2 pressures and the filament temperatures were 1.3 kPa and room temperature (○), 1.3 kPa and 2700 K (□), and 2.7 kPa and 2700 K (●).

Similar plots could be obtained under other conditions, and the rotational temperatures are summarized in Table I. The rotational temperature when the filament was not heated was determined to be 310±30 K, while those when the filament temperature was 2700 K were more than 1000 K in the presence of more than 670 Pa of H_2. The error limits in the rotational temperatures are standard deviations.

Our data analysis procedure of the CARS spectra was similar to those employed by Chen et al.,[28] Shaub et al.,[33] and Andrews et al.[37] In general, the CARS signal intensity is proportional to the products of the square of the third-order nonlinear susceptibility $\chi^{(3)}$, the Stokes laser pulse intensity, and the square of the pump laser intensity. The pump laser intensity at 532 nm was fixed during the measurements. The Stokes laser intensity was around 10% weaker at shorter wavelength. The wavelength dependence was corrected in Fig. 1. The third-order nonlinear susceptibility $\chi^{(3)}$ can be expressed by a function of J and ν. It should be noted that $\chi^{(3)}$ depends little on J but is proportional to $\nu+1$. In other words, the sensitivity to detect $H_2(\nu=1)$ is four times larger than for $H_2(\nu=0)$. Strictly speaking, the signal intensity depends on both the line-shape functions of the lasers and on a

factor that in turn depends on the frequencies and the focusing conditions.[34] However, these factors were not taken into account in the present analysis. The error caused by such ignorance must be small since we could obtain a room-temperature rotational distribution when the filament was not heated. In general, in CARS measurements, only the population difference between the two molecular levels, such as $[H_2(\nu+1)]-[H_2(\nu)]$, can be determined. However, since the signal intensity corresponding to $H_2(\nu=1)$ was much smaller than that corresponding to $H_2(\nu=0)$, the contribution of the $\nu=1$ level was ignored in the evaluation of the population of the $\nu=0$ level, while that of the $\nu=2$ level was ignored in the evaluation of the $\nu=1$ level population.

CARS signals corresponding to $H_2(\nu=1,J=1)$ and $H_2(\nu=1,J=3)$ could be identified at 3917 and 3888 cm^{-1}, respectively, as shown in Fig. 1. Other signals, such as those attributable to $J=2$ or $J=5$, were below the detection limit. The relative population of $H_2(\nu=1)$ and $H_2(\nu=0)$ was evaluated from the populations of the $J=1$ and $J=3$ levels by assuming the same rotational temperatures for the $\nu=0$ and $\nu=1$ states. The results are summarized in Table I. It is rather difficult to evaluate the error limits for the vibrational population ratios, but ±20% may be inevitable. If we extrapolate the population ratios to typical CVD pressure conditions, such as 10 Pa, the population of $H_2(\nu=1)$ is estimated to be 0.7±0.2% of that for $H_2(\nu=0)$. Under typical filament temperatures for Cat-CVD, such as 2000 K, this population ratio should be much less.

We also tried to determine the rotational and the vibrational distributions by reducing the distance between the filament and the detection zone to 2 cm. The relative population of $H_2(\nu=1)$ was slightly higher than it was at 5 cm. For example, it was 0.014 when the filament temperature was 2700 K and the H_2 pressure was 670 Pa. However, it was found that the rotational Boltzmann plots are nonlinear. Similar results were obtained at other pressure conditions. The spatial distribution of rotationally excited H_2 must have been inhomogeneous.

It might be considered that only part of the H_2 introduced into the chamber collides with the filament, and this is

TABLE I. Rotational and vibrational population distributions of diatomic molecules in catalytic decomposition systems. nd: vibrationally excited levels were not detected. rt: room temperature.

Source gas	Species detected	Filament temperature (K)	Filament/detection zone distance (cm)	Total pressure	Rotational temperature (K)	$\nu=1/\nu=0$ ratio	Reference
H_2	H_2	2700	5	67 Pa	700±30	nd	
H_2	H_2	2700	5	130 Pa	770±40	nd	
H_2	H_2	2700	5	670 Pa	1030±40	0.009	
H_2	H_2	2700	5	1.3 kPa	1140±30	0.010	
H_2	H_2	2700	5	2.0 kPa	1170±30	0.010	
H_2	H_2	2700	5	2.7 kPa	1200±40	0.015	Present
H_2	H_2	2500	5	1.3 kPa	1100±20	nd	
H_2	H_2	2500	5	2.0 kPa	1070±20	nd	
H_2	H_2	rt		27 Pa	310±30	nd	
H_2	H_2	rt		1.3 kPa	310±30	nd	
SiH_4/H_2	SiH	2300	10	6.7 Pa	390±40	nd	31
NH_3	NH	2300	10	20 Pa	500±50	nd	32
HCN	CN	2300	10	1.3 Pa	350	0.23	30

TABLE II. Rotational and vibrational distributions of H_2 in hot filament excitation.

Detection technique	Filament temperature/ electric power	Filament/detection zone distance (cm)	Total pressure	Rotational temperature (k)	$\nu=1/\nu=0$ ratio (vibrational temperature)	Reference
CARS	2820 K/2 kW	0.65	2.7 kPa	1590		28
H^- monitoring	1770 K		6.7 Pa	700	0.002 (960 K)	29
CARS	2373 K	0.4	4.7 kPa (0.5% CH_4)	1600		12
CARS	2700 K/3.0 kW	5	2.7 kPa	1200	0.015 (1420 K)	Present
			67 Pa	700	0.007[a] (1200 K)	

[a]Extrapolated value.

IV. DISCUSSION

the reason for the low population of $H_2(\nu=1)$. However, this is not the case. It is possible to estimate how many times a hydrogen molecule collides with the filament before being evacuated. Since the area of the filament was 2.7×10^{-3} m^2, the number of collisions in unit time in the presence of 1.3 kPa of H_2, 9.4×10^{22} m^{-3} at 10^3 K, is 2.0×10^{23} s^{-1}. The H_2 flow rate was 100 SCCM, that is, 4.2×10^{19} s^{-1}. This ratio, 5×10^3, should be a measure of the number of collisions. Although the above is a rough estimation, it may be concluded that all the molecules introduced collide with the filament many times before being evacuated.

Tables II and III summarize the rotational temperature and the ratio of the $H_2(\nu=1)$ population to that of $H_2(\nu=0)$ in hot filament and plasma excitation. Although the state distributions must depend on the experimental conditions, such as the chamber geometry and total pressure, it can be concluded that the $H_2(\nu=1)/H_2(\nu=0)$ population ratio is smaller in hot filament excitation than in plasma excitation. Table IV compares the vibrational temperatures for highly excited levels, $\nu\geqslant2$. The temperature for plasma excitation is not necessarily higher than that for hot filament excitation in this case.

The cause of the vibrational excitation of H_2 has been discussed extensively. In hot filament excitation, it is now well recognized that the highly vibrationally excited levels are produced on the chamber walls by a recombination process. Eenshuistra et al. found that the vibrational population ratio $[H_2(\nu=5)]/[H_2(\nu=4)]$ depends little on the filament temperature and concluded that the direct production of highly vibrationally excited H_2 on a hot filament is minor.[38] They have proposed the Eley-Rideal process, in which $H_2(\nu)$ is formed by the recombination of H atoms adsorbed on the surface with those coming from the gas phase. Their conclusion was further supported by Schermann et al., who showed that the vibrational state distribution remains constant when the filament temperature is changed.[29] Schermann et al. also proposed the presence of a physisorbed H-atom layer on the chemisorbed one to explain the high vibrational excitation. This Eley-Rideal mechanism has also been supported by theoretical calculations.[39] In plasma, similar excitation processes must also be possible,[25] although collisional activation by electrons of energies in excess of 10 eV must also play some roles.[23]

The production processes of the first excited level, $H_2(\nu=1)$, on the other hand, may be different. In plasma excitation, it has been proposed that low energy electrons, whose kinetic energy is less than 1 eV, collide with unexcited molecules to generate vibrational excitation.[19,20] This mechanism is consistent with the present result that the $[H_2(\nu=1)]/[H_2(\nu=0)]$ population ratio is smaller in the hot filament excitation where no free electrons are present. If low vibrational states such as $H_2(\nu=1)$ are also produced by the recombination of two H atoms, the vibrational population ratio $[H_2(\nu=1)]/[H_2(\nu=0)]$ should be higher in hot filament excitation than in plasma, since more H atoms are expected to be produced in hot filament excitation. This is not the case as is shown in Tables II and III. The low vibrational states in plasma processes must be produced by collisions with subexcited electrons. On hot filaments, dissociation to two H atoms should be more predominant than vibrational excitation for H_2. The vibrational temperature of CN radicals produced by the catalytic decomposition of HCN is higher than those of H_2 observed in the present work, although the filament temperature was lower.[30] This may be because CN

TABLE III. Rotational and vibrational distributions of H_2 in plasma excitation.

Detection technique	Electric power/ voltage/current	Total pressure	Rotational temperature (k)	$\nu=1/\nu=0$ ratio (vibrational temperature)	Reference
CARS	90 V/10 A	5.5 Pa	530	0.082 (2390 K)	19
REMPI	100 V/10 A	1.2 Pa	390	0.090 (2480 K)	20
CARS	37.5 A	40 Pa	800[a]	0.037[a] (1800 K)	22
			1380[b]	0.091[b] (2500 K)	
CARS	0.5 W cm^{-3}	200 Pa	600	0.22 (3980 K)	26
	2.0 W cm^{-3}	1.07 kPa	800	0.14 (3000 K)	

[a]Axial position: 150 mm.
[b]Axial position: 25 mm.

TABLE IV. Vibrational distributions of $H_2(\nu \geq 2)$ in plasma and hot filament excitation. VUV means vacuum ultraviolet.

Excitation technique	Detection technique	Total pressure	Vibrational temperature over $\nu=2$ level	Reference
plasma (90 V, 10 A)	CARS	5.5 Pa	2390 K	19
plasma (125 V, 25 A)	VUV absorption	1.1 Pa	4180 K	21
plasma (100 V, 0.5 A)	LIF	1.5 Pa	non-Boltzmann $\approx 11\,000$ K	23
plasma (60 A, 9 kW)	LIF	13 kPa[a]	2200 K	24
plasma (1 eV)	LIF	20 Pa	2600 K	25
hot filament (2500 K, 4 V, 15 A)	H^- monitoring	0.01 Pa	non-Boltzmann ≈ 3000 K	27
hot filament (1770 K)	H^- monitoring	6.7 Pa	3900 K	29

[a]Pressure at the plasma source.

bonds are not broken on hot filaments and the vibrational excitation does not compete with the bond dissociation. In addition, CN radicals may deposit on chamber walls with a high efficiency and the vibrational temperature may be frozen. On the other hand, $H_2(\nu)$ must be deactivated without deposition.

The decrease not only in the rotational temperature but also in the vibrational temperature with the decrease in the H_2 pressure, as is shown in Table I, suggests the importance of the relaxation processes on chamber walls, which were water cooled. Collisional relaxation in the gas phase may play some roles but is less important. This is consistent with the small rate constant for the vibrational relaxation of $H_2(\nu)$ by H_2.[40] Although the rate constant increases exponentially with temperature, the rate constant at 1000 K is still in the order of 10^{-15} cm^3 s^{-1}.[41] The rate constant for the vibrational relaxation by H is rather large because this may proceed via a chemical atom-transfer process, $H + H_2(\nu=1) \rightarrow H_2(\nu=0) + H$.[42,43] However, the H-atom density may not be enough for this process to be important. Another possible explanation to the total pressure dependence of the rotational and vibrational temperatures is the contribution of termolecular H-atom recombination processes in the gas phase. The recombination rate of two H atoms to produce rotationally and vibrationally excited H_2 molecules must be larger at higher pressures, although the termolecular rate constant is rather small, 3.8×10^{-33} cm^6 s^{-1} at 1200 K.[44] However, if this is the case, as has been discussed above, more excitation is expected in hot filament than in plasma. The much lower vibrational temperature in the present system suggests that the recombination processes in the gas phase are less important.

V. CONCLUSIONS

The vibrational population ratio $[H_2(\nu=1)]/[H_2(\nu=0)]$ in hot filament excitation is much lower than those observed in hydrogen plasma, even when the filament temperature is as high as 2700 K. The recombination reactions of two H atoms on the chamber walls may be important to produce highly vibrationally excited H_2 but are not important in the production of $H_2(\nu=1)$. Under typical catalytic CVD conditions, no vibrationally excited H_2 molecules are expected to play any roles. This is in contrast to plasma processes, in which the interaction between subexcited electrons and

$H_2(\nu=0)$ contributes to the production of $H_2(\nu=1)$ and the high-density $H_2(\nu=1)$ molecules may also play a role.

[1]H. Matsumura, Jpn. J. Appl. Phys., Part 1 **37**, 3175 (1998).
[2]H. Matsumura, H. Umemoto, A. Izumi, and A. Masuda, Thin Solid Films **430**, 7 (2003).
[3]H. Matsumura, H. Umemoto, and A. Masuda, J. Non-Cryst. Solids **338–340**, 19 (2004).
[4]A. M. Wrobel, S. Wickramanayaka, and Y. Hatanaka, J. Appl. Phys. **76**, 558 (1994).
[5]A. M. Wróbel, A. Walkiewicz-Pietrzykowska, Y. Hatanaka, S. Wickramanayaka, and Y. Nakanishi, Chem. Mater. **13**, 1884 (2001).
[6]J. T. Herron, J. Phys. Chem. Ref. Data **28**, 1453 (1999).
[7]H. Umemoto, R. Ozeki, M. Ueda, and M. Oku, J. Chem. Phys. **117**, 5654 (2002).
[8]H. Umemoto and M. Oku, Bull. Chem. Soc. Jpn. **76**, 291 (2003).
[9]K. P. Huber and G. Herzberg, *Constants of Diatomic Molecules, Molecular Spectra and Molecular Structure* Vol. IV. (Van Nostrand Reinhold, New York, 1979).
[10]H. Umemoto, K. Ohara, D. Morita, Y. Nozaki, A. Masuda, and H. Matsumura, J. Appl. Phys. **91**, 1650 (2002).
[11]U. Meier, K. Kohse-Hoinghaus, L. Schafer, and C.-P. Klages, Appl. Opt. **29**, 4993 (1990).
[12]L. L. Connell, J. W. Fleming, H.-N. Chu, D. J. Vestyck, Jr., E. Jensen, and J. E. Butler, J. Appl. Phys. **78**, 3622 (1995).
[13]A. Rousseau, A. Granier, G. Gousset, and P. Laprince, J. Phys. D **27**, 1412 (1994).
[14]A. D. Tserepi and T. A. Miller, J. Appl. Phys. **75**, 7231 (1994).
[15]A. Kubo, M. Kitajima, M. Yata, and H. Fukutani, Jpn. J. Appl. Phys., Part 1 **39**, 6101 (2000).
[16]J. Jolly and J.-P. Booth, J. Appl. Phys. **97**, 103305 (2005).
[17]G. C. Light, J. Chem. Phys. **68**, 2831 (1978).
[18]G. P. Glass and B. K. Chaturvedi, J. Chem. Phys. **75**, 2749 (1981).
[19]M. Péalat, J-P. E. Taran, M. Bacal, and F. Hillion, J. Chem. Phys. **82**, 4943 (1985).
[20]J. H. M. Bonnie, P. J. Eenshuistra, and H. J. Hopman, Phys. Rev. A **37**, 1121 (1988).
[21]G. C. Stutzin, A. T. Young, H. F. Döbele, A. S. Schlachter, K. N. Leung, and W. B. Kunkel, Rev. Sci. Instrum. **61**, 619 (1990).
[22]R. F. G. Meulenbroeks, R. A. H. Engeln, J. A. M. van der Mullen, and D. C. Schram, Phys. Rev. E **53**, 5207 (1996).
[23]T. Mosbach, H.-M. Katsch, and H. F. Döbele, Phys. Rev. Lett. **85**, 3420 (2000).
[24]P. Vankan, D. C. Schram, and R. Engeln, J. Chem. Phys. **121**, 9876 (2004).

[25] P. Vankan, D. C. Schram, and R. Engeln, Chem. Phys. Lett. **400**, 196 (2004).

[26] V. A. Shakhatov, O. De Pascale, M. Capitelli, K. Hassouni, G. Lombardi, and A. Gicquel, Phys. Plasmas **12**, 023504 (2005).

[27] R. I Hall, I. Čadež, M. Landau, F. Pichou, and C. Schermann, Phys. Rev. Lett. **60**, 337 (1988).

[28] K.-H. Chen, M.-C. Chuang, C. M. Penney, and W. F. Banholzer, J. Appl. Phys. **71**, 1485 (1992).

[29] C. Schermann, F. Pichou, M. Landau, I. Čadež, and R. I Hall, J. Chem. Phys. **101**, 8152 (1994).

[30] H. Umemoto, T. Morimoto, M. Yamawaki, Y. Masuda, A. Masuda, and H. Matsumura, J. Non-Cryst. Solids **338–340**, 65 (2004).

[31] Y. Nozaki, K. Kongo, T. Miyazaki, M. Kitazoe, K. Horii, H. Umemoto, A. Masuda, and H. Matsumura, J. Appl. Phys. **88**, 5437 (2000).

[32] H. Umemoto, K. Ohara, D. Morita, T. Morimoto, M. Yamawaki, A. Masuda, and H. Matsumura, Jpn. J. Appl. Phys., Part 1 **42**, 5315 (2003).

[33] W. M. Shaub, J. W. Nibler, and A. B. Harvey, J. Chem. Phys. **67**, 1883 (1977).

[34] D. P. Gerrity and J. J. Valentini, J. Chem. Phys. **81**, 1298 (1984).

[35] T. Morimoto, H. Umemoto, K. Yoneyama, A. Masuda, H. Matsumura, K. Ishibashi, H. Tawarayama, and H. Kawazoe, in Nano Electronic Materials, special issue of Jpn. J. Appl. Phys., Part 1 **44**, 732 (2005).

[36] S. G. Ansari, H. Umemoto, T. Morimoto, K. Yoneyama, A. Izumi, A. Masuda, and H. Matsumura, Thin Solid Films (in press).

[37] B. K. Andrews, K. A. Burton, and R. B. Weisman, J. Chem. Phys. **96**, 1111 (1992).

[38] P. J. Eenshuistra, J. H. M. Bonnie, J. Los, and H. J. Hopman, Phys. Rev. Lett. **60**, 341 (1988).

[39] B. Jackson and M. Persson, J. Chem. Phys. **96**, 2378 (1992).

[40] S. K. Pogrebnya and D. C. Clary, Chem. Phys. Lett. **363**, 523 (2002).

[41] D. R. Flower and E. Roueff, J. Phys. B **31**, 2935 (1998).

[42] D. R. Flower and E. Roueff, J. Phys. B **31**, L955 (1998).

[43] O. Dobis and S. W. Benson, J. Phys. Chem. A **106**, 4403 (2002).

[44] D. L. Baulch *et al.*, J. Phys. Chem. Ref. Data **21**, 411 (1992).